MRI and Spectroscopy for Characterization of Primary Human Mutant IDH1 (IDH1-R132H) Glioblastoma Xenografts

Yanping Sun[1], Shakti Ramkissoon[2], Matthew A Theisen[2], Amy S Freund[3], Kristen L Jones[1], Marika Hayashi[2], Juan Wang[1], Keith Ligon[2], and Andrew L Kung[1,4]

[1]Lurie Family Imaging Center, Dana-Farber Cancer Institute, Boston, MA, United States, [2]Center for Molecular Oncologic Pathology, Dana-Farber Cancer Institute, [3]Bruker BioSpin Corp., Billerica, [4]Pediatric Oncology, Children's Hospital, Boston

Introduction

Gliomas are the most common and invariably fatal primary adult brain tumors. Studies have been performed to define sub-classes of gliomas, and to identify oncogenic alterations for the development of new targeted treatments. Mutations in isocitrate dehydrogenase 1 and 2 (IDH1/2) and excessive production of the onco-metabolite 2-hydroxyglutarate (2HG) have been found in adult low grade gliomas and secondary glioblastomas (GBMs) (1). To evaluate the effects of drug candidates inhibiting the IDH enzyme, an animal model is essential. In this study, we developed an intracranial primary xenograft GBM model harboring the IDH1-R132H mutation. *In vivo* MRI was used to monitor tumor growth and characterization; *ex vivo* MRS was used to study the metabolite spectrum with presence of 2HG in the tumor.

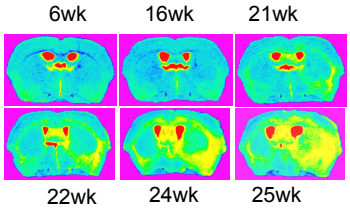

Fig.1. Tumor growth over time by MRI

Methods

GBM Xenograft Model and Histologic Analysis*:* A primary GBM cell line (BT116) expressing IDH1-R132H mutation was derived from surgical resection material acquired from a patient undergoing surgery on an IRB approved protocol. Tumor resected samples were mechanically dissociated and cell viability was assessed by trypan blue exclusion prior to stereotactic injection. SCID (IcrTac:ICR-Prkdcscid) mice were injected with 20,000 viable cells in the right striatum. At the onset of neurological symptoms, mice were euthanized and cardiac perfused with 4% PFA prior to removal of the brain, which was then sectioned for paraffin embedding, H&E staining, immunohistochemistry for IDH1-R132H and histologic examination.

In vivo MR Scans*:* Mice bearing IDH1 mutant brain tumor xenografts were imaged every 3 weeks to monitor tumor development, and thereafter weekly. The MRI experiments were carried out on a Bruker 7T MRI system. Mice were anesthetized with 1-1.5% isoflurane in medical air. T2 weighted images were acquired to follow tumor growth with RARE sequence. T1, T2 and perfusion were acquired for characterization of the IDH tumor using IR, MSME and FAIR-RARE methods.

Ex vivo 1H HR-MAS*:* After *in vivo* MRI imaging, IDH-mutant tumor tissue were collected from 4 mice, snap frozen in liquid nitrogen and stored at –80°C. Tissue samples were placed in a 80μL disposable rotor insert, and then into a ceramic 4mm rotor. A small amount of D2O was added for lock. HR-MAS was acquired using a Bruker 500 MHz spectrometer at a temperature of 278k, 2250 Hz spin rate in an inverse TXI HR-MAS probe. A 1D presaturation sequence was run with 1s acquisition time (AQ), 1s relaxation delay (D1), 128 scans (NS), 20k acquired points (TD), 10kHz spectral width. A 2D adiabatic-TOCSY was performed to further obtain 2HG information. The data were analyzed using Bruker TopSpin. Bruker's AMIX software was used to identify metabolites. For comparison purposes, 1D spectrum and 2D TOCSY data were obtained from one brain tumor sample without IDH mutation.

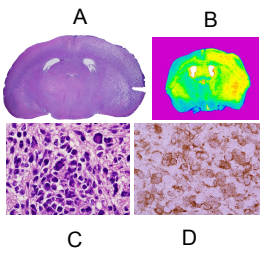

Fig.2. Comparison of MRI and histologic findings

Results: Fig. 1 demonstrates the slow progression of the IDH-mutant GBM over time. MRI performed at 6 week post-injection showed no detectable tumor; however, by 16 weeks a minimal tumor burden was identified at the injection site. MRIs performed at 21 and 22 weeks showed tumor progression characterized by infiltrative growth throughout the right hemisphere in a ring-like distribution eventually resulting in a left-sided midline shift noted at 24 weeks. By week 25, the right hemisphere was extensively involved by tumor particularly evident in the right striatum, right cortex, bilateral periventricular regions and right corpus callosum with prominent extension into the left hemisphere along white matter tracts. Consistent with other types of brain tumors, the T1 and T2 value in tumor (T1t and T2t) were significantly larger than normal brain tissue (T1n and T2n): T1t=1656±50ms, T1n=1409±47ms, with p=0.0005; T2t=60±4ms, T2n=47±1ms, with p=0.002. Tumor perfusion was lower than normal tissue with an average reduction of 54% ±8%. Fig. 2 demonstrates the histological correlates to MRI imaging of BT116 xenografts. A coronal brain section (H&E) of the BT116 xenograft (Fig. 2A) shows a diffusely infiltrating neoplasm predominantly involving the right hemisphere with expansion of the periventricular regions and corpus callosum, which is in consistent with the pattern observed by MRI (Fig. 2B). At higher magnification (Figs. 2C-D, 100x), the tumor is characterized as a densely cellular glial neoplasm composed of large pleomorphic cells which are positive by immunohistochemistry for the mutant form of IDH1 (IDH1-R132H). Fig 3A shows 1D spectrum where 2HG peaks are present at 4.04ppm, 2.26ppm, 2.0ppm, and 1.84ppm in IDH-mutant tumor, but absent in control tumor. 2D TOCSY in Fig. 3B further confirmed the presence of 2HG (resonances highlighted with black rectangular) in IDH tumor but absent in control tumor. These findings are consistent with the presence of 2HG in IDH1 mutated glioma in patients (2, 3).

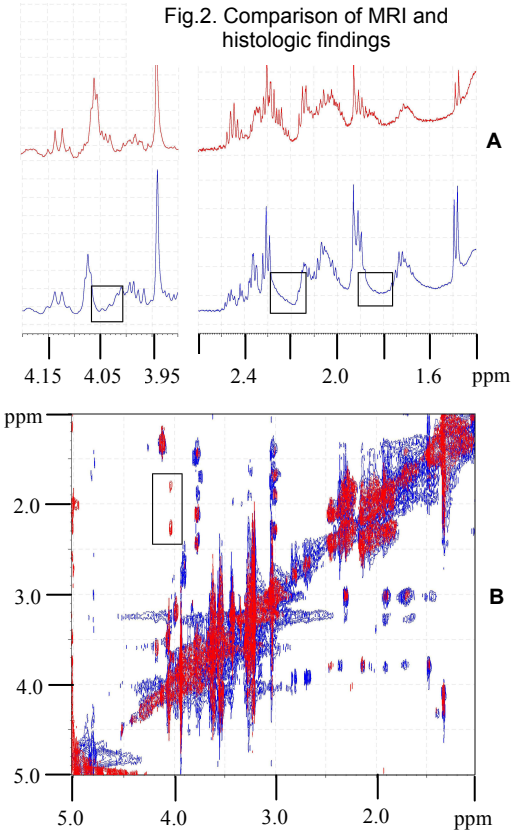

Fig.3. 1D and 2D Spectrum of IDH Tumor (red) and control tumor (blue)

Conclusions: The growth pattern and characterization of primary human mutant IDH1 glioblastoma observed by MRI were consistent with histologic findings in our animal model. Further, MRS of tumors with IDH1 mutations revealed the presence of 2HG which were not seen in a tumor with germline IDH1. MRI and MRS are powerful tools for non-invasively monitoring tumor growth and detecting 2HG in animal models, which may serve as a biomarker in development of novel drugs inhibiting the function of IDH mutant.

References : [1] Yan, *et al*. (2009) NEJM 360: 765-73. [2] Jalbert, *et al*. (2011) Proc. Intl. Soc. Mag. Reson. Med. 19: 183. [3] Elkhaled, *et al*. (2011) Proc. Intl. Soc. Mag. Reson. Med. 19: 182.